ACS MATERIALS LETTERS

www.acsmaterialsletters.org

LETTER

Low-Defect, High Molecular Weight Indacenodithiophene (IDT) Polymers Via a C−H Activation: Evaluation of a Simpler and Greener Approach to Organic Electronic Materials

James F. Ponder Jr,* Hu Chen, Alexander M. T. Luci, Stefania Moro, Marco Turano, Archie L. Hobson, Graham S. Collier, Luís M. A. Perdigão, Maximilian Moser, Weimin Zhang, Giovanni Costantini, John R. Reynolds, and Iain McCulloch

Cite This: *ACS Materials Lett.* 2021, 3, 1503−1512

Read Online

ACCESS | Metrics & More | Article Recommendations | Supporting Information

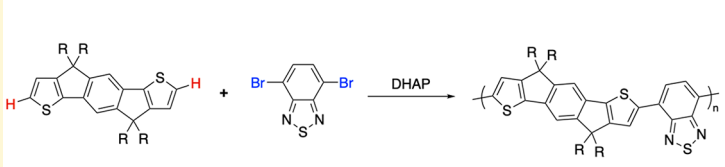

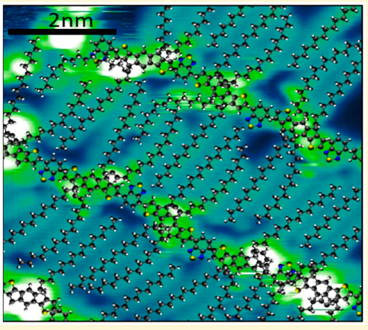

ABSTRACT: **The development, optimization, and assessment of new methods for the preparation of conjugated materials is key to the continued progress of organic electronics. Direct C−H activation methods have emerged and developed over the last 10 years to become an invaluable synthetic tool for the preparation of conjugated polymers for both redox-active and solid-state applications. Here, we evaluate direct (hetero)arylation polymerization (DHAP) methods for the synthesis of indaceno[1,2-b:5,6-b′]dithiophene-based polymers. We demonstrate, using a range of techniques, including direct visualization of individual polymer chains via high-resolution scanning tunneling microscopy, that DHAP can produce polymers with a high degree of regularity and purity that subsequently perform in organic thin-film transistors comparably to those made by other cross-coupling polymerizations that require increased synthetic complexity. Ultimately, this work results in an improved atom economy by reducing the number of synthetic steps to access high-performance molecular and polymeric materials.**

As research into the properties and application of organic semiconducting polymers has progressed over the past several decades, the need for simple and reliable polymerization methods has become increasingly important. Currently, Migita-Kosugi-Stille (Stille)[1−3] and Suzuki-Miyaura (Suzuki)[4] polymerizations are the leading methods for the preparation of soluble conjugated copolymers. However, both of these methods have limitations that increase the complexities of the synthesis and hinder the development of new materials. Suzuki polymerizations require the preparation of boronic esters that can undergo protodeborylation[5] (as monomers or during polymerization) and typically cannot be purified by column chromatography. On the one hand, these units are hydrolyzed in situ during the polymerization,[6,7] and an optimization of this hydrolysis via a base choice is typically required for an effective cross-coupling.[8,9] Stille polymerizations, on the other hand, are

Received: August 8, 2021
Published: September 16, 2021

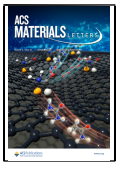

Scheme 1. Synthetic Outline of IDT-BT Prepared using Suzuki, Stille, or DHAP Conditions

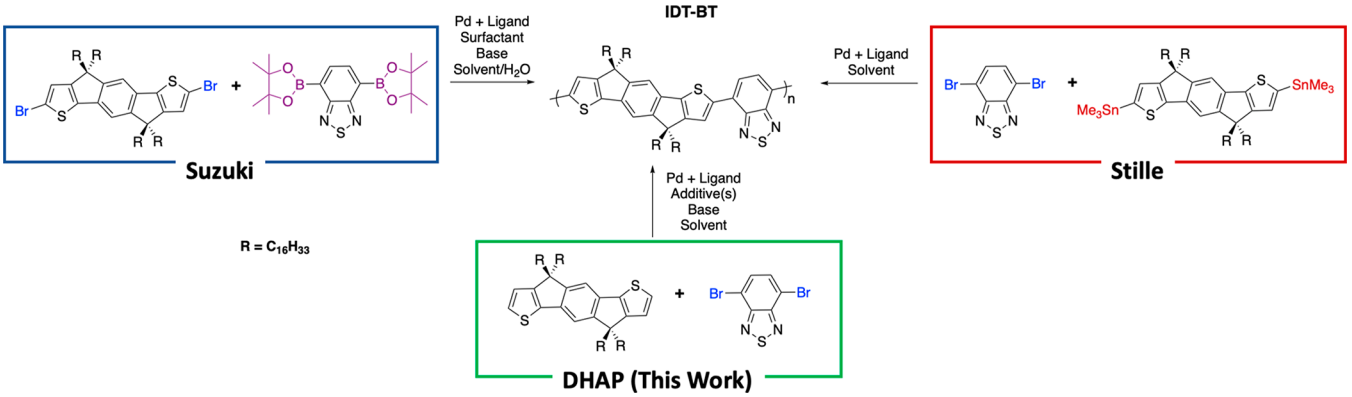

relatively simple, and optimization is typically not required to obtain high molecular weight polymers, making this a preferred method for the development of new materials.[10] Unfortunately, the trialkyltin monomers often suffer from poor stability, can be difficult to purify, and are prepared from highly toxic trialkyltin halides[11] that are regenerated as byproducts[2,3,12,13] during reactions. It also has been demonstrated that, even after extensive purification, residual tin remains in the final conjugated polymers.[14]

Since the initial application of direct C−H activation toward the synthesis of organic semiconductors, first used to prepare oligomeric thiophenes in 1999[15] and further exploited to prepare polymers in 2010,[16] this method has received significant attention due to the simpler monomer preparation compared to the Stille and Suzuki reactions, lack of excessively toxic intermediates and byproducts, and more recently, the use of environmentally benign and/or renewable solvents.[17−22] Direct (hetero)arylation polymerization (DHAP, also termed DArP) has become the standard method for the preparation of dioxyheterocycle polymers for redox-active applications[23−25] and has even been demonstrated to produce polymers with an applicability in organic photovoltaics (OPVs) that show a comparable power conversion efficiency (PCE) to polymers synthesized via Stille cross-couplings.[20,26,27] DHAP also has been found to be relatively insensitive to atmospheric oxygen and tolerant to water, with truly anhydrous conditions inhibiting an effective polymerization unless additional base is added.[28] The high dielectric solvent reaction conditions (e.g., DMF, NMP, or DMAc as a solvent) favored for dioxythiophenes (XDOTs) and phenylenes increase the catalytic turnover, resulting in rapid polymerizations. However, this increased polarity also increases the reactivity of C−H bonds on heteroaromatic β-carbons, which can result in branched or cross-linked polymer chains, making these conditions unsuitable for monomers with unprotected reactive sites. Here we focus on the conditions needed to make polymers of thiophene-based cores and exclude dioxyheterocycles[23] that cannot form branching defects. In these cases, low-dielectric solvents (e.g., toluene, xylenes, chlorobenzene, or tetrahydrofuran (THF)) are used, typically with additional additives, to yield low-defect materials.[29] Several "greener" solvents (e.g., 2-MeTHF or *p*-cymene)[19,30] also have been found to be effective for these reactions.

Over the past decade indaceno[1,2-b:5,6-b′]dithiophene (IDT) copolymers have become ubiquitous in the field of organic thin-film transistors (OTFTs).[31] Of particular note is the alternating donor−acceptor (D-A) copolymer of IDT bearing *n*-hexadecyl side chains with 2,1,3-benzothiadiazole (BT).[32,33] This polymer, termed IDT-BT, has provided a standard for the development of new high-mobility *p*-type polymers. Since its development, a variety of derivatives have been reported varying the fused core, side chains, and acceptor comonomer, leading to OTFT hole mobility (μ_h) values approaching 3 $cm^2/(V\ s)$ in optimized devices.[31,34] While IDT-BT is typically prepared via Suzuki polymerizations, as shown in Scheme 1, the majority of other polymers using IDT-based cores are prepared using Stille polymerizations.[31,35] The IDT unit, typically with *n*-octyl, 2-ethylhexyl, or *p*-(*n*-hexyl)-phenyl side chains, also serves as a key building block for discrete molecular acceptors used in OPVs[36] and is conventionally prepared via either a Stille or Suzuki reaction.

Here, we report that high molecular weight IDT-BT can be prepared via DHAP with a comparable OTFT performance to batches synthesized via Suzuki methods, with OTFT hole mobilities exceeding 2 $cm^2/(V\ s)$. Simple polymerization conditions are used with a select few variations to evaluate how variables, such as precatalyst, ligand, or coligand, influence molecular weight, cross-coupling defects, and, ultimately, device properties. A discussion of different DHAP conditions and how the reagents used in this work were selected is included to provide insight for those intending to use DHAP. Various methods, including high-resolution scanning tunneling microscopy (STM) imaging, are used to elucidate the polymer structures. Finally, we demonstrate that the simple C−H activation conditions reported here can be used to prepare IDT-based acceptor cores used for OPVs, simplifying the synthesis for the development of high-performance conjugated polymers, new molecular acceptors, and, subsequently, industrial scale-up.

As a means to initially assess our C−H activation methodology with the IDT core, we utilized C−H activation for the synthesis of discrete acceptor molecules (often termed non-fullerene acceptors (NFAs) in the literature) typically used in OPV and OTFT applications. Currently, IDT-based small molecules represent a significant fraction of state-of-the-art acceptor materials for OPV[37] and have found additional application in organic photodetectors[38] and OTFTs.[39] These materials are generally prepared by stannylation of the IDT core[40] or bromination of IDT and borylation[41] of the complementary acceptor reactant. This introduces additional synthetic steps using toxic reagents to yield intermediates that can be difficult to purify. Here, we apply a simple C−H activation methodology previously used to synthesize ion-sensing molecules[42] to prepare a commonly studied acceptor

https://doi.org/10.1021/acsmaterialslett.1c00478
ACS Materials Lett. 2021, 3, 1503−1512

Scheme 2. (a) Synthesis of an IDT-Based Molecular Acceptor Model System and (b) Synthesis of IDT-BT Via Suzuki and DHAP[a]

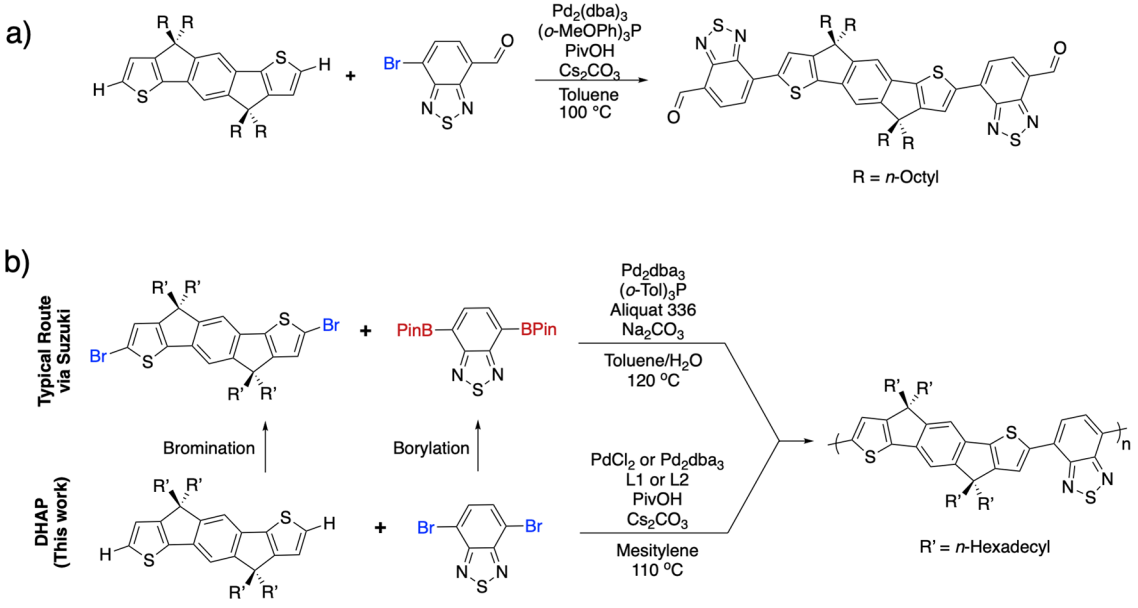

[a]In the DHAP conditions: L1 = $(o\text{-MeOPh})_3P$, and L2 = $(o\text{-MeOPh})_3P$ + TMEDA.

Table 1. Synthetic and Molecular Weight Information for the IDT-BT Batches

				GPC			STM		
polymer	catalyst	ligand	reaction yield (%)	M_n (kg/mol)[a]	M_w (kg/mol)[a]	$Đ$[b]	M_n (kg/mol)	M_w (kg/mol)	$Đ$[b]
Suz-M	Pd_2dba_3	$(o\text{-Tol})_3P$	89	61	117	1.9	39	49	1.3
DHAP-L	$PdCl_2$	$(o\text{-MeOPh})_3P$	33	22	28	1.3	19	24	1.3
DHAP-M	Pd_2dba_3	$(o\text{-MeOPh})_3P$ + TMEDA	96	71	209	2.9	39	42	1.1
DHAP-H	Pd_2dba_3	$(o\text{-MeOPh})_3P$	94	79	214	2.7	41	52	1.3

[a]Estimated vs polystyrene standards in TCB at 140 °C. [b]$Đ = M_w/M_n$.

core. As detailed in the Supporting Information and shown in Scheme 2a, *n*-octyl functionalized IDT was coupled to commercially available 7-bromo-2,1,3-benzothiadiazole-4-carboxaldehyde with a high yield of 86% in one step. This protocol demonstrates a significant reduction in the synthetic complexity of OPV acceptor units via direct arylation methods and provides an initial set of conditions to be used for polymerizations.

IDT-BT batches (referred to as DHAP-L, DHAP-M, and DHAP-H for low-, medium-, and high-molecular weight batches, respectively) were prepared, as shown in Scheme 2, using conditions described in detail in the Supporting Information and briefly discussed here. The solvent, proton transfer shuttle, and base were kept constant in this work, as these play more subtle roles in the polymerization, while the precatalyst and ligand systems were manipulated to yield the different DHAP batches, as shown in Table 1. The conventional proton transfer shuttle and base pair of pivalic acid and cesium carbonate were selected due to their broad use in DHAP. Mesitylene was chosen as the low-dielectric solvent for this study, as it has been reported to be less reactive and yields higher molecular weight polymers compared to other common aromatic solvents[43] and was found to effectively dissolve IDT-BT. A total monomer concentration was maintained at 0.1−0.2 M to balance reaction kinetics and effective solvation of the growing polymer chains. Palladium(0) and palladium(II) precatalysts both have been used in DHAP to prepare high-performance materials. While the Pd(II) precatalysts, namely, $Pd(OAc)_2$ and Herrmann's catalyst, are most commonly used, $PdCl_2$[44,45] was selected for this work, as it has been reported that the free Cl^- anion can improve the M_n of resulting polymers compared to $Pd(OAc)_2$. Tris(dibenzylideneacetone)-dipalladium(0) (Pd_2dba_3) is the Pd(0) precatalyst of choice for C−H activation, as tetrakis(triphenylphosphine)-palladium(0) ($Pd(PPh_3)_4$) has repeatedly been found to be ineffective for this methodology. Pd_2dba_3 and $PdCl_2$ were used to produce DHAP-H and DHAP-L, respectively. While ligands are typically not used for DHAP in high-dielectric solvents, ligands are generally needed when using a low-dielectric and noncoordinating media to more effectively solubilize the Pd complex. Tris(*o*-methoxyphenyl)phosphine [$(o\text{-MeOPh})_3P$] was selected as the ligand, as it has been found highly effective in a C−H activation reaction for small molecules[42,46] and polymers.[47,48] The diamine *N,N,N′,N′*-tetramethylethylenediamine (TMEDA) has been reported to function as a coligand with $(o\text{-MeOPh})_3P$ in DHAP reactions, yielding increased polymer molecular weights by suppressing side reactions.[49,50] Motivated by these reports, the TMEDA "mixed-ligand" system was evaluated in conjunction with Pd_2dba_3 to produce DHAP-M.

The polymers were purified via precipitation into methanol followed by a Soxhlet washing with methanol, acetone, and hexanes, and finally dissolution into chloroform followed by a reprecipitation and a wash with methanol, as detailed in the Supporting Information. The yields of the polymerization, in terms of the $CHCl_3$-soluble and isolated fractions, varied significantly based on the Pd precatalyst used, with a low yield of

https://doi.org/10.1021/acsmaterialslett.1c00478
ACS Materials Lett. 2021, 3, 1503−1512

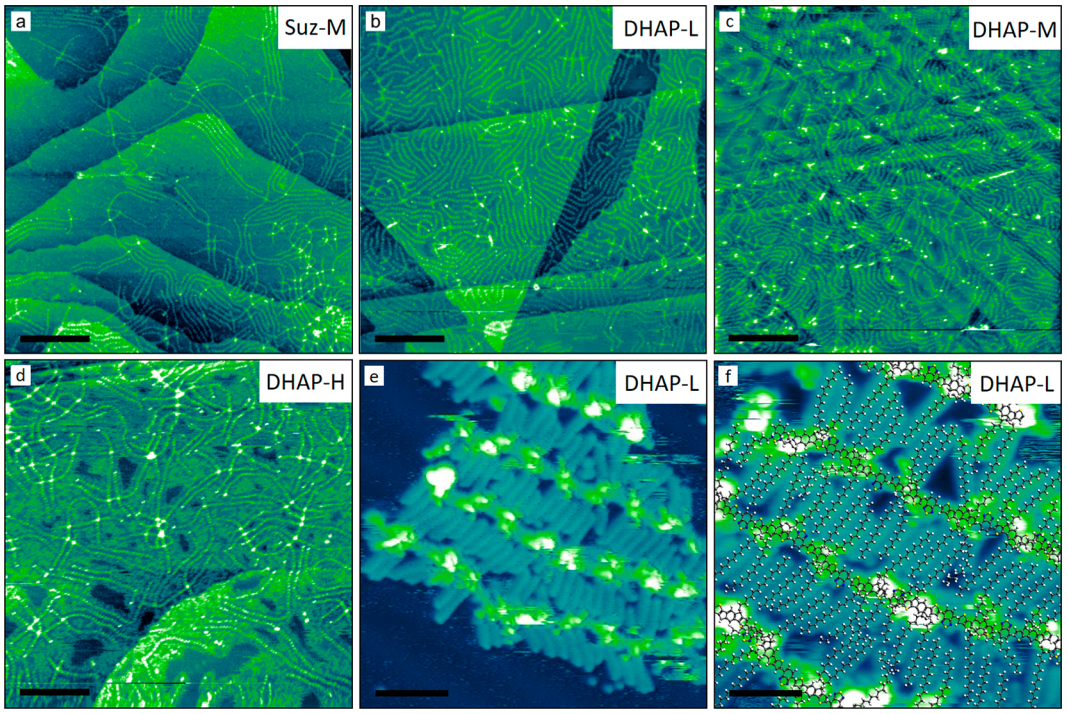

Figure 1. STM images of (a) Suz-M, (b) DHAP-L, (c) DHAP-M, and (d) DHAP-H IDT-BT polymers deposited in vacuum by ESD on a Au(111) substrate. (e) High-resolution STM image of a self-assembled island of DHAP-L, showing a region with several parallel arranged macromolecules and highly interdigitated side chains. (f) Enlarged area of (e) with a superposed molecular model. Images (a−d) were acquired at −145 °C with a sample bias between −1.5 and −1.3 V and a tunneling current between 30 and 50 pA; images (e, f) at −196 °C with a sample bias of −1.0 and +1.0 V, respectively, and a tunneling current of 90 pA. The black scale bars correspond to 40 nm (a−d), 3 nm (e), and 2 nm (f).

33% for DHAP-L and excellent yields of 96% and 94% for DHAP-M and DHAP-H, respectively. The lower yield observed from DHAP-L is due to a significant amount of the material, presumably lower molecular weight oligomer/polymer chains, being removed in Soxhlet fractions (primarily hexanes) prior to the extraction of the polymer in chloroform. The composition of the polymers was probed using elemental analysis and was found to slightly vary from the expected values for DHAP-L and DHAP-M, while matching the expected values for DHAP-H, as listed with the synthetic details in the Supporting Information. From this we can expect some structural variation in DHAP-L and DHAP-M from the proposed polymer repeat units. The structure of the repeat unit was further probed and confirmed via ^{1}H NMR, as shown in Figure S1.

The number and weight average molecular weight (M_n and M_w, respectively) and molecular weight dispersity ($Đ = M_w/M_n$) of the of the polymers, listed in Table 1, were estimated using gel permeation chromatography (GPC) with 1,2,4-trichlorobenzene (TCB) as the eluent relative to narrow molecular weight polystyrene standards, shown in Figure S2. These polymers were compared to a representative batch of IDT-BT of medium molecular weight prepared via a Suzuki polymerization (Suz-M), with molecular weight information also listed in Table 1. Both of the DHAP batches prepared using the Pd(0) precatalyst are comparable to Suz-M in terms of molecular weight, albeit with broader dispersities. The use of TMEDA does not, in this case, increase the M_n of the polymer and actually lowers the M_n relative to the exact same conditions without it. The Pd(II) precatalyst resulted in a lower molecular weight polymer, as expected, due to the stoichiometric imbalance introduced from a homocoupling of the IDT units to produce the active Pd(0) catalyst. This type of homocoupling has been directly observed for XDOT copolymers prepared using a Pd(II) catalyst in DHAP via matrix-assisted laser desorption/ionization (MALDI) mass spectrometry.[51] Additionally, the lower yield and M_n of DHAP-L suggest that the reported benefit of Cl^- anions is not generally applicable.

The molecular weights of the polymers also were examined by using a recently developed methodology that utilizes electrospray deposition (ESD) coupled with ultrahigh-vacuum STM to image polymers at a high spatial resolution[52] and determine their length distribution.[53,54] The resulting molecular weight distributions are reported in Figure S3, and the corresponding M_n values are listed in Table 1. While the trend in M_n is consistent between the two methods used for molecular weight estimation, the GPC results indicate higher molecular weights than those observed via STM. It has been previously noted that GPC measurements can overestimate molecular weights[55] for conjugated polymers due to various factors including aggregation. While the STM analysis should not be affected by these factors, it could however be biased toward lower molecular weights, due to a combination of lower solubility of longer polymers and the finite size of the images used in evaluating the M_n values (see the Supporting Information).

Irrespective of the polymerization method and the precatalyst used in DHAP, individual polymers appear as flexible, elongated structures that occasionally display high-curvature bends, as seen in representative STM images of the different polymer batches (Figure 1a−d). For all four batches, the molecular chains adsorb face-on onto the Au(111) substrate and, despite the absence of long-range order,[56] they locally tend to align parallel to each other, particularly in the regions of higher molecular density. DHAP-L polymers form two-dimensional (2D) films that are visually more compact and ordered (Figure

https://doi.org/10.1021/acsmaterialslett.1c00478
ACS Materials Lett. 2021, 3, 1503−1512

1b) than their higher-M_n counterparts (Figures 1c,d). This behavior is largely ascribable to an average shorter length that facilitates the parallel arrangement of the polymers with respect to the DHAP-M and DHAP-H batches.

Scheme S1 provides the structures of theoretical defects that could potentially be formed during the DHAP synthesis. In DHAP, a homocoupling of the dibromide species (Scheme S1a) is not expected based on the catalytic cycle, but a homocoupling of the dihydrogen species (Scheme S1b) is expected to occur in equal quantity to the catalyst loading when using a Pd(II)-based catalyst, and it could potentially be found in greater abundance if an oxidant (e.g., O_2) is present in the reaction media.[57,58] Finally, branching of the polymer chain (Scheme S1c), referred to as a β-defect, is caused by an unselective C−H activation. This is typically observed when using a high-dielectric solvent, or when a bromine atom is adjacent to an active C−H bond. By using mesitylene as the solvent and the molecular design of the IDT and BT comonomers, an observation of β-defects is not expected in this study under the selected reaction conditions.

To find possible indications of defects, multiple STM images were analyzed. If present, polymer chain branching should be apparent in large-scale images as the splitting of a single polymer strand into two existing branches. No evidence of this behavior was observed in any of the samples studied. There are a few cases where four polymer strands can be seen emerging from the same position, but the use of higher magnification reveals this to be a crossing point between two individual, regular polymer chains. Although not very frequently, these crossings can indeed result from the random deposition of the macromolecules onto the gold surface. Because the observed crossings invariably involve four strands, they should not be mistaken for actual branching points of the polymers' backbones. If these crossings corresponded to branching defects, a connectivity between three strands would be visualized (see Scheme S1c). Moreover, in all of the observed crossings, a brighter protrusion is typically recognizable at the position of overlap, indicating a locally higher surface topography, which is what is expected as two polymer chains cross one another (see Figure S4 as an example).

To establish the occurrence of the other two types of potential polymerization defects, highly resolved images are needed to sequence individual molecular units along the backbones, as previously reported.[53] Such a resolution has been achieved in the case of the more ordered DHAP-L batch, as shown in Figure 1e. The polymer backbones display a periodic sequence of bright protrusions (average separation 1.6 ± 0.1 nm), each of which is caused by the two nonplanar sp^3 bridging quaternary carbons in the IDT units. The solubilizing side chains appear as paired elongated structures extending perpendicular from the backbones and interdigitating with the side chains of neighboring polymers in a way that bears some analogies with the assembly expected in solid-state thin films.[59] While the relatively high density of quaternary carbon atoms makes it difficult to attain the resolution needed to directly sequence the polymers, the location of the IDT subunits can be estimated from the bright protrusions along the backbone and from the exit position of the alkyl chains with respect to the backbone. With this methodology, as shown in Figure 1f, it is possible to construct a molecular model that satisfactorily fits the STM image, showing that the DHAP-L polymer chains are mostly defect-free. Only in an extremely small number of cases have we managed to detect locations along the backbones, where the distances between successive IDT subunits appeared to be smaller than the regular ones (see Figure 2). In these instances, a satisfactory molecular

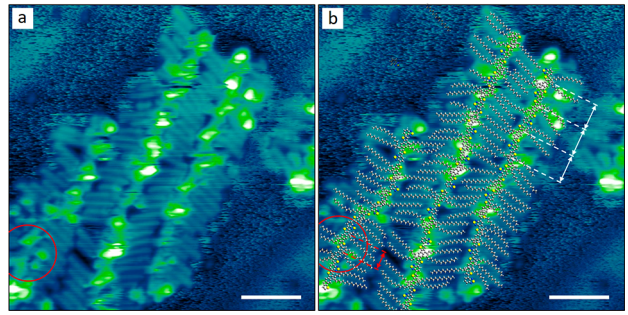

Figure 2. (a) High-resolution STM image of a high-density region of the DHAP-L polymer; (b) same area of (a) with a superposed molecular model. The red circles indicate the position of a dihydrogen homocoupling polymerization defect, appearing like a fourfold clover in STM. The double arrows in (b) indicate the separation between successive polymer subunits for a regular polymer (white) and for a polymer with a homocoupling (red). The image was acquired at a sample temperature of −196 °C with a tunneling current I = 60 pA and a sample bias voltage V_{bias} = +1.25 V. The white scale bars correspond to 3 nm.

modeling could only be attained by assuming that two successive IDT subunits were directly connected to each other without any BT subunit in between (see Figure 2b); in other words, these defects correspond to dihydrogen homocouplings (Scheme S1b), as is expected in trace amounts when using a Pd(II) precatalyst. As far as can be determined by an examination of high-resolution images, the few observed defects account for less than 1% of the total analyzed monomer couplings and consist only of occasional examples of dihydrogen homocouplings. Details of the defect analysis are reported in Table S2.

Proton (^{1}H) nuclear magnetic resonance (NMR) spectroscopy is another useful method for probing polymer structures for defects. As seen in Figure 3a, the aromatic region of the spectra shows the same dominant peaks for all DHAP batches and Suz-M. The spectrum of DHAP-L shows several additional peaks, denoted with *, between 7.70 and 8.10 ppm. These peaks (ca. 8.08, 7.88, and 7.79 ppm) can be attributed to terminal BT units based on their chemical shifts and splitting patterns. A visualization of these terminal units is indicative of a low M_n polymer and a relatively higher fraction of chain ends. The IDT β-proton peak, centered at ∼7.43 ppm, shows a clear shoulder that could also be the result of end IDT units; however, the overlap of these peaks limits a definitive determination. All of these features are absent in the DHAP-M and -H spectra, which is attributed to their higher molecular weights. No homocoupling defects are observed in the DHAP batches; however, due to the breadth of polymer NMR peaks it is impossible to definitively say there is no homocoupling based on these results. The spectrum of Suz-M shows a doublet at ∼7.91 ppm, indicated by a + sign. While the origin of this proton shift is unclear, the fact it is unique to the Suz-M suggests it is the proton resulting from a protodeborylation of terminal BT units.

UV−Vis absorbance spectroscopy shows nearly identical absorption profiles between the polymers prepared from different methods. As seen in Figure 3b, there is minimal difference between the higher-weight batches from DHAP and the Suz-M batch, which is indicative of all of the polymers reaching sufficiently high molecular weights to achieve saturated electronic properties. DHAP-L shows a slight tailing of the absorption profile at low energy, potentially due to the previously noted homocoupling of IDTs. An electrochemical

https://doi.org/10.1021/acsmaterialslett.1c00478
ACS Materials Lett. 2021, 3, 1503−1512

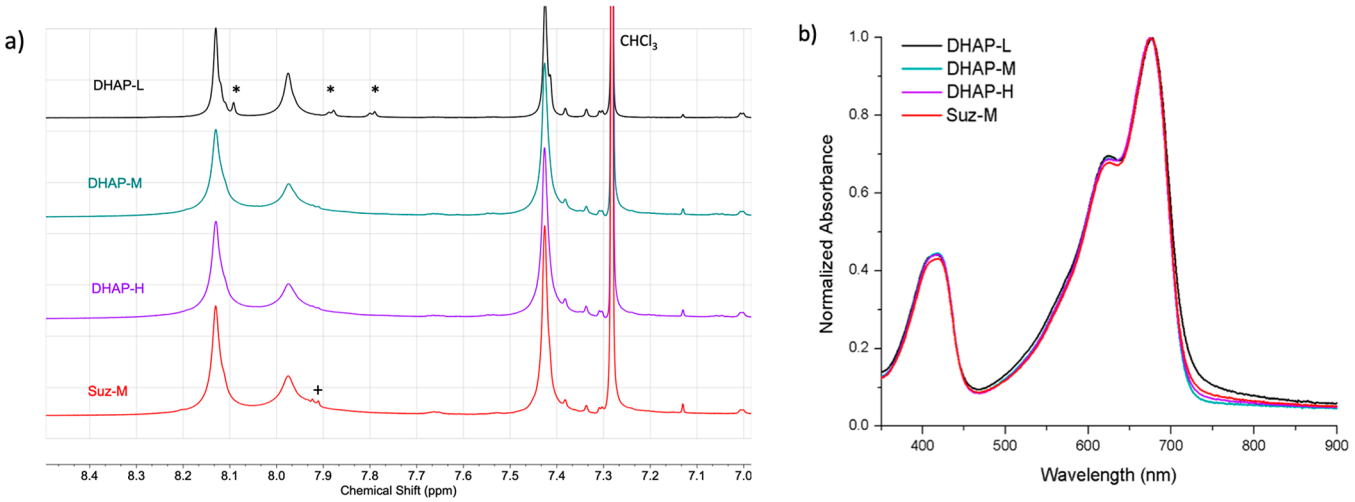

Figure 3. (a) ^{1}H NMR spectra of the aromatic region of the polymers in $CDCl_3$, showing potential end groups with * and unknown defects with +. (b) UV−Vis spectra of films of the IDT-BT batches on glass.

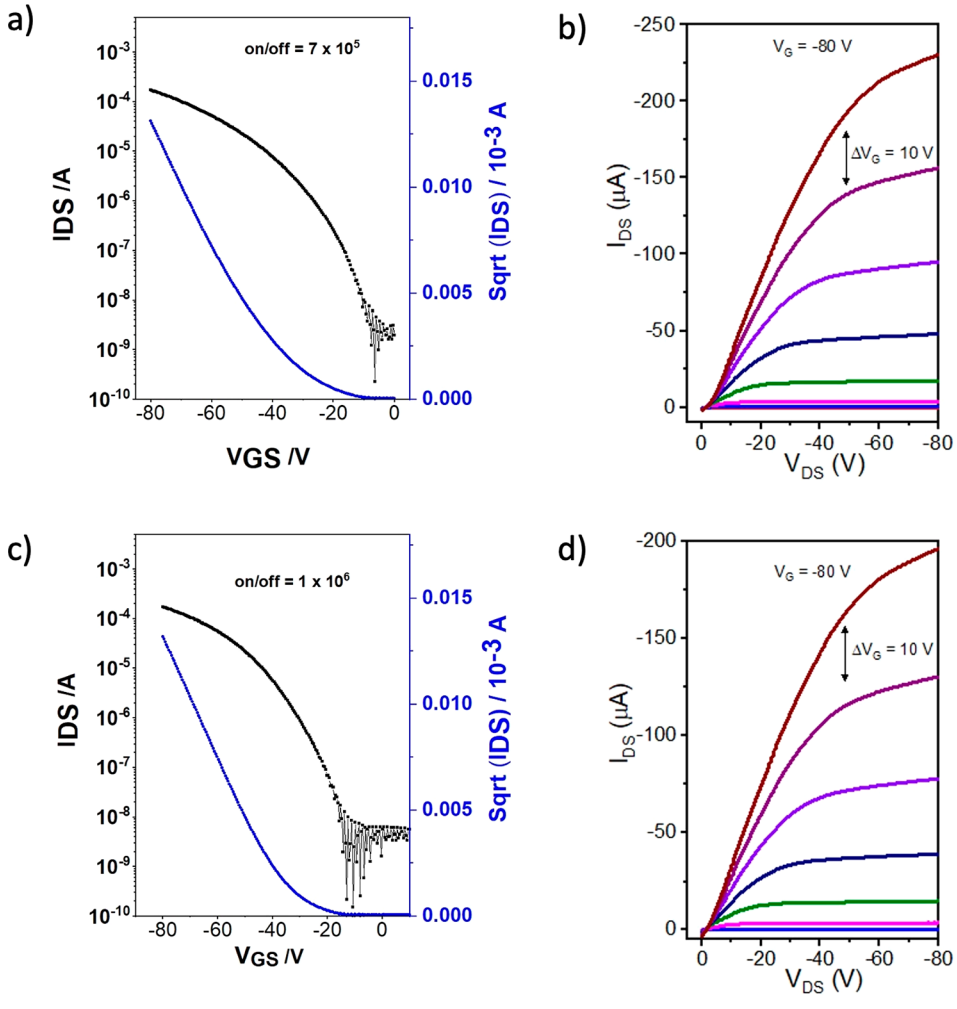

Figure 4. (a) Representative saturation transfer and (b) output characteristics for Suz-H OTFT devices. (c) Representative saturation transfer and (d) output characteristics for DHAP-H OTFT devices.

analysis of the polymers shows larger variations between batches. From the cyclic voltammograms (CVs) of the polymer films, shown in Figure S6, it can be seen that there is almost no difference between the DHAP-H, DHAP-M, and Suz-M. DHAP-L shows a similar behavior, but with less resolved oxidation and reduction features.

The performance of each polymer was evaluated in OTFT devices. Initial IDT-BT samples were found to have μ_h of ∼1 $cm^2/(V\,s)$, and an optimization of molecular weight and device

https://doi.org/10.1021/acsmaterialslett.1c00478
ACS Materials Lett. 2021, 3, 1503−1512

architecture has produced devices with μ_h as high as ~3 $cm^2/(V\ s)$.[32,56] The molecular weight of a polymer can have either a dramatic or minimal effect on the electronic properties of a system depending on both the specific polymer backbone and the application of interest. Many redox-active polymers, such as dioxythiophenes,[25] do not show significant molecular weight dependencies above an initial low M_n, while other systems, such as poly(3-hexylthiophene),[60,61] show clear molecular weight trends for a range of applications. As the mobility of IDT-BT is known to be sensitive to molecular weight,[56] two additional batches prepared via Suzuki were also assessed. From the transfer and output characteristics of the polymers, shown in Figure 4 for DHAP-H and Suz-H and in Figure S7 for the remaining polymers, it can be seen that the DHAP materials compare favorably to those synthesized via Suzuki polymerizations. As seen in Table 2, all of the polymers demonstrated a high μ_h, indicative of low-defect materials, as the OTFT device performance is sensitive to impurities and/or polymer defects. While the Suzuki batches show on/off ratios ranging from 10^4 to 10^6, the DHAP batches are all on the order of 10^6. This could potentially be due to a higher purity of the polymers, fewer coupling defects, or the lack of residual boronic ester/acid functionalities on polymer chain ends.

Table 2. Summary of IDT-BT OTFT Device Performance for All Suzuki and DHAP Batches

Polymer	μ_h ($cm^2/(V\ s)$)	V_{th} (V)	I_{on}/I_{off}
Suz-L	0.5 ± 0.06	−19 ± 1.5	2×10^6
Suz-M	1.9 ± 0.3	−10 ± 2.2	5×10^4
Suz-H	2.6 ± 0.2	−30 ± 0.7	7×10^5
DHAP-L	0.8 ± 0.07	−8 ± 1.4	1×10^6
DHAP-M	1.6 ± 0.4	−18 ± 2.7	3×10^6
DHAP-H	2.3 ± 0.1	−33 ± 2.3	1×10^6

As seen in Figure 5, the various batches of IDT-BT show the expected trend of increasing mobility with M_n, for this system. Because of the relatively low crystallinity of IDT-BT, the magnitude of the $Đ$ does not seem to affect the observed trend.

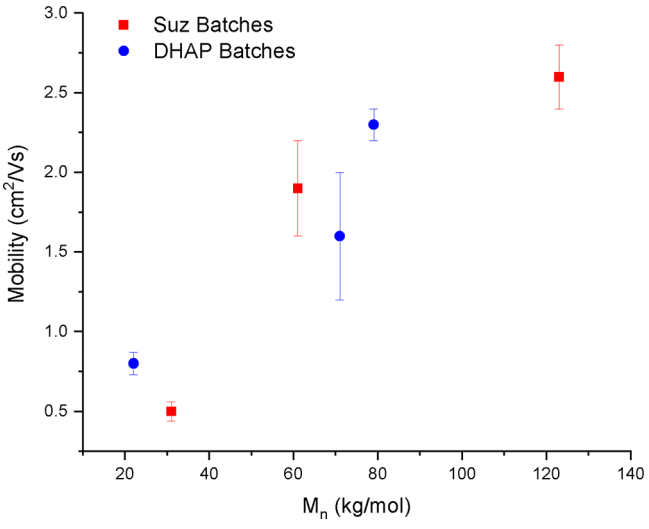

Figure 5. Mobility of IDT-BT OTFTs as a function of molecular weight, as determined by GPC, for both Suzuki (red) and DHAP (blue) batches, with error bars representing one standard deviation from the mean across more than 10 devices.

While the M_n of DHAP-H is ~40 kg/mol lower than that of Suz-H, the mobilities of the samples are within error of each other, indicating a statistically insignificant difference in values and demonstrating that polymers prepared via DHAP can match those produced by other methods.

In summary, we show that simple DHAP conditions can produce high molecular weight and high-purity copolymers with an OTFT performance that is comparable to that of batches prepared from more traditionally used methods. Reagent selection can be used to control the molecular weight of IDT-BT, with a catalyst system prepared from a Pd(0) precatalyst and electron-rich phosphine ligand providing the highest weight and highest mobility material. The introduction of a diamine coligand was found to be unnecessary for this class of monomers, with a slightly higher M_n observed when TMEDA was omitted from the reaction. The previously observed benefit of free chloride ions in solution, relative to acetate, could not overcome the drawbacks of using a Pd(II) precatalyst, with the polymer prepared by this route having the lowest synthetic yield, M_n, and OTFT mobility. Further research will be needed to determine if free chloride ions used in conjunction with a Pd(0) precatalyst could yield improved results.

STM imaging confirms the GPC trends in the mass distributions and indicates that the polymers contain minimal defects. High-resolution NMR spectra do not show any clear defects in the polymers prepared using DHAP, and elemental analysis shows excellent agreement between the theoretical values and those obtained experimentally for the optimized DHAP batch (namely, DHAP-H). This finding expands the scope and ease of development for new high-mobility fused polymers. Additionally, as the IDT unit is the benchmark core for discrete acceptor molecules,[62,37,36] this methodology can reduce the synthetic complexity of acceptor synthesis, which will be vital for a large-scale commercialization of OPVs.[63] However, it is important to emphasize that, while a C−H activation has demonstrated significant progress in regards to the scope of monomers amendable to DHAP polymerization conditions, several challenges still remain. A few select monomers show poor C−H bond selectivity even when using optimized conditions, resulting in polymer chain branching and/or chain cross-linking. Additionally, some monomers (e.g., thiophene or furan) have low boiling points that limit their implementation in DHAP. In these situations, methods such as Stille, Suzuki, and Grignard metathesis (GRIM) should be considered as potentially more productive routes.

■ ASSOCIATED CONTENT

Supporting Information

The Supporting Information is available free of charge at https://pubs.acs.org/doi/10.1021/acsmaterialslett.1c00478.

Materials, polymerization conditions, characterizations, and instrumentation details (PDF)

■ AUTHOR INFORMATION

Corresponding Author

James F. Ponder Jr − *George W. Woodruff School of Mechanical Engineering, Georgia Institute of Technology, Atlanta 30332 Georgia, United States;* orcid.org/0000-0001-8093-1849; Email: jponder7@gatech.edu

https://doi.org/10.1021/acsmaterialslett.1c00478
ACS Materials Lett. 2021, 3, 1503−1512

Authors

Hu Chen − *KAUST Solar Center, Physical Sciences and Engineering Division, King Abdullah University of Science and Technology, Thuwal 23955-6900, Saudi Arabia;* orcid.org/0000-0001-8426-4254

Alexander M. T. Luci − *Department of Chemistry, University of Warwick, Coventry CV4 7AL, U.K.*

Stefania Moro − *Department of Chemistry, University of Warwick, Coventry CV4 7AL, U.K.;* orcid.org/0000-0001-8445-4509

Marco Turano − *Department of Chemistry, University of Warwick, Coventry CV4 7AL, U.K.*

Archie L. Hobson − *Department of Chemistry, University of Warwick, Coventry CV4 7AL, U.K.;* orcid.org/0000-0001-7548-8299

Graham S. Collier − *Department of Chemistry and Biochemistry, Kennesaw State University, Kennesaw 30144 Georgia, United States;* orcid.org/0000-0002-9650-8110

Luís M. A. Perdigão − *Department of Chemistry, University of Warwick, Coventry CV4 7AL, U.K.;* orcid.org/0000-0002-0534-1512

Maximilian Moser − *Department of Chemistry, Chemistry Research Laboratory, University of Oxford, Oxford OX1 3TA, U.K.;* orcid.org/0000-0002-3293-9309

Weimin Zhang − *KAUST Solar Center, Physical Sciences and Engineering Division, King Abdullah University of Science and Technology, Thuwal 23955-6900, Saudi Arabia*

Giovanni Costantini − *Department of Chemistry, University of Warwick, Coventry CV4 7AL, U.K.;* orcid.org/0000-0001-7916-3440

John R. Reynolds − *School of Chemistry and Biochemistry, School of Materials Science and Engineering, Center for Organic Photonics and Electronics, Georgia Tech Polymer Network, Georgia Institute of Technology, Atlanta 30332 Georgia, United States;* orcid.org/0000-0002-7417-4869

Iain McCulloch − *Department of Chemistry, Chemistry Research Laboratory, University of Oxford, Oxford OX1 3TA, U.K.;* orcid.org/0000-0002-6340-7217

Complete contact information is available at: https://pubs.acs.org/10.1021/acsmaterialslett.1c00478

Notes

The authors declare no competing financial interest.

■ ACKNOWLEDGMENTS

JFP would like to thank Abigail A. Advincula for assistance in electrochemical measurements and Dr. Austin L. Jones for assistance in GPC measurements. The authors acknowledge financial support from KAUST, including Office of Sponsored Research (OSR) awards no. OSR-2018-CRG/CCF-3079, OSR-2019-CRG8-4086 and OSR-2018-CRG7-3749. The authors acknowledge funding from ERC Synergy Grant SC2 (610115), the European Union's Horizon 2020 research and innovation program under grant agreement no. 952911, project BOOSTER and grant agreement no. 862484, project RoLAFLEX, as well as EPSRC Project EP/T026219/1. G.C. acknowledges financial support from the University of Warwick. A.M.T.L. and M.T. gratefully acknowledge financial support from the Engineering and Physical Sciences Research Council (EPSRC) grant EP/L015307/1 for the Molecular Analytical Science Centre for Doctoral Training (MAS-CDT). S.M. acknowledges funding though an EU Chancellor's Scholarship by the University of Warwick. G.S.C and J.R.R acknowledges funding from the Office of Naval Research (N00014-20-1-2129).

■ REFERENCES

(1) Azarian, D.; Dua, S. S.; Eaborn, C.; Walton, D. R. M. Reactions of organic halides with R3MMR3 compounds (M = Si, Ge, Sn) in the presence of tetrakis(triarylphosphine)palladium. *J. Organomet. Chem.* **1976**, *117*, C55−C57.

(2) Kosugi, M.; Sasazawa, K.; Shimizu, Y.; Migita, T. Reactions of allyltin compounds Iii. Allylation of aromatic halides With allyltributyltin in the presence of tetrakis (triphenylphosphine) palladium (O). *Chem. Lett.* **1977**, *6*, 301−302.

(3) Milstein, D.; Stille, J. A general, selective, and facile method for ketone synthesis from acid chlorides and organotin compounds catalyzed by palladium. *J. Am. Chem. Soc.* **1978**, *100*, 3636−3638.

(4) Miyaura, N.; Yanagi, T.; Suzuki, A. The Palladium-Catalyzed Cross-Coupling Reaction of Phenylboronic Acid with Haloarenes in the Presence of Bases. *Synth. Commun.* **1981**, *11*, 513−519.

(5) Leone, A. K.; Mueller, E. A.; McNeil, A. J. The History of Palladium-Catalyzed Cross-Couplings Should Inspire the Future of Catalyst-Transfer Polymerization. *J. Am. Chem. Soc.* **2018**, *140*, 15126−15139.

(6) Knapp, D. M.; Gillis, E. P.; Burke, M. D. A General Solution for Unstable Boronic Acids: Slow-Release Cross-Coupling from Air-Stable MIDA Boronates. *J. Am. Chem. Soc.* **2009**, *131*, 6961−6963.

(7) Thomas, A. A.; Denmark, S. E. Pre-transmetalation intermediates in the Suzuki-Miyaura reaction revealed: The missing link. *Science* **2016**, *352*, 329−332.

(8) Murage, J.; Eddy, J. W.; Zimbalist, J. R.; McIntyre, T. B.; Wagner, Z. R.; Goodson, F. E. Effect of Reaction Parameters on the Molecular Weights of Polymers Formed in a Suzuki Polycondensation. *Macromolecules* **2008**, *41*, 7330−7338.

(9) Carrillo, J. A.; Turner, M. L.; Ingleson, M. J. A General Protocol for the Polycondensation of Thienyl N-Methyliminodiacetic Acid Boronate Esters To Form High Molecular Weight Copolymers. *J. Am. Chem. Soc.* **2016**, *138*, 13361−13368.

(10) Carsten, B.; He, F.; Son, H. J.; Xu, T.; Yu, L. Stille Polycondensation for Synthesis of Functional Materials. *Chem. Rev.* **2011**, *111*, 1493−1528.

(11) Kimbrough, R. D. Toxicity and health effects of selected organotin compounds: a review. *Environ. Health Perspect.* **1976**, *14*, 51−56.

(12) Espinet, P.; Echavarren, A. M. The Mechanisms of the Stille Reaction. *Angew. Chem., Int. Ed.* **2004**, *43*, 4704−4734.

(13) Cordovilla, C.; Bartolomé, C.; Martínez-Ilarduya, J. M.; Espinet, P. The Stille Reaction, 38 Years Later. *ACS Catal.* **2015**, *5*, 3040−3053.

(14) Lo, C. K.; Gautam, B. R.; Selter, P.; Zheng, Z.; Oosterhout, S. D.; Constantinou, I.; Knitsch, R.; Wolfe, R. M. W.; Yi, X.; Brédas, J.-L.; So, F.; Toney, M. F.; Coropceanu, V.; Hansen, M. R.; Gundogdu, K.; Reynolds, J. R. Every Atom Counts: Elucidating the Fundamental Impact of Structural Change in Conjugated Polymers for Organic Photovoltaics. *Chem. Mater.* **2018**, *30*, 2995−3009.

(15) Sévignon, M.; Papillon, J.; Schulz, E.; Lemaire, M. New synthetic method for the polymerization of alkylthiophenes. *Tetrahedron Lett.* **1999**, *40*, 5873−5876.

(16) Wang, Q.; Takita, R.; Kikuzaki, Y.; Ozawa, F. Palladium-Catalyzed Dehydrohalogenative Polycondensation of 2-Bromo-3-hexylthiophene: An Efficient Approach to Head-to-Tail Poly(3-hexylthiophene). *J. Am. Chem. Soc.* **2010**, *132*, 11420−11421.

(17) Mercier, L. G.; Leclerc, M. Direct (Hetero)Arylation: A New Tool for Polymer Chemists. *Acc. Chem. Res.* **2013**, *46*, 1597−1605.

(18) Suraru, S.-L.; Lee, J. A.; Luscombe, C. K. C-H Arylation in the Synthesis of π-Conjugated Polymers. *ACS Macro Lett.* **2016**, *5*, 724−729.

(19) Pankow, R. M.; Ye, L.; Gobalasingham, N. S.; Salami, N.; Samal, S.; Thompson, B. C. Investigation of green and sustainable solvents for direct arylation polymerization (DArP). *Polym. Chem.* **2018**, *9*, 3885−3892.

(20) Dudnik, A. S.; Aldrich, T. J.; Eastham, N. D.; Chang, R. P. H.; Facchetti, A.; Marks, T. J. Tin-Free Direct C-H Arylation Polymerization for High Photovoltaic Efficiency Conjugated Copolymers. *J. Am. Chem. Soc.* **2016**, *138*, 15699−15709.
(21) Bura, T.; Blaskovits, J. T.; Leclerc, M. Direct (Hetero)arylation Polymerization: Trends and Perspectives. *J. Am. Chem. Soc.* **2016**, *138*, 10056−10071.
(22) Stepek, I. A.; Itami, K. Recent Advances in C-H Activation for the Synthesis of π-Extended Materials. *ACS Materials Letters* **2020**, *2*, 951−974.
(23) Estrada, L. A.; Deininger, J. J.; Kamenov, G. D.; Reynolds, J. R. Direct (Hetero)arylation Polymerization: An Effective Route to 3,4-Propylenedioxythiophene-Based Polymers with Low Residual Metal Content. *ACS Macro Lett.* **2013**, *2*, 869−873.
(24) Savagian, L. R.; Österholm, A. M.; Ponder, J. F., Jr; Barth, K. J.; Rivnay, J.; Reynolds, J. R. Balancing Charge Storage and Mobility in an Oligo(ether) Functionalized Dioxythiophene Copolymer for Organic- and Aqueous- Based Electrochemical Devices and Transistors. *Adv. Mater.* **2018**, *30*, 1804647.
(25) Österholm, A. M.; Ponder, J. F.; De Keersmaecker, M.; Shen, D. E.; Reynolds, J. R. Disentangling Redox Properties and Capacitance in Solution-Processed Conjugated Polymers. *Chem. Mater.* **2019**, *31*, 2971−2982.
(26) Aldrich, T. J.; Zhu, W.; Mukherjee, S.; Richter, L. J.; Gann, E.; DeLongchamp, D. M.; Facchetti, A.; Melkonyan, F. S.; Marks, T. J. Stable Postfullerene Solar Cells via Direct C-H Arylation Polymerization. Morphology-Performance Relationships. *Chem. Mater.* **2019**, *31*, 4313−4321.
(27) Mainville, M.; Leclerc, M. Direct (Hetero)arylation: A Tool for Low-Cost and Eco-Friendly Organic Photovoltaics. *ACS Applied Polymer Materials* **2021**, *3*, 2.
(28) Grenier, F.; Goudreau, K.; Leclerc, M. Robust Direct (Hetero)arylation Polymerization in Biphasic Conditions. *J. Am. Chem. Soc.* **2017**, *139*, 2816−2824.
(29) Gobalasingham, N. S.; Thompson, B. C. Direct arylation polymerization: A guide to optimal conditions for effective conjugated polymers. *Prog. Polym. Sci.* **2018**, *83*, 135−201.
(30) Ye, L.; Thompson, B. C. p-Cymene: A Sustainable Solvent that is Highly Compatible with Direct Arylation Polymerization (DArP). *ACS Macro Lett.* **2021**, *10*, 714−719.
(31) Wadsworth, A.; Chen, H.; Thorley, K. J.; Cendra, C.; Nikolka, M.; Bristow, H.; Moser, M.; Salleo, A.; Anthopoulos, T. D.; Sirringhaus, H.; McCulloch, I. Modification of Indacenodithiophene-Based Polymers and Its Impact on Charge Carrier Mobility in Organic Thin-Film Transistors. *J. Am. Chem. Soc.* **2020**, *142*, 652−664.
(32) Zhang, W.; Smith, J.; Watkins, S. E.; Gysel, R.; McGehee, M.; Salleo, A.; Kirkpatrick, J.; Ashraf, S.; Anthopoulos, T.; Heeney, M.; McCulloch, I. Indacenodithiophene Semiconducting Polymers for High-Performance, Air-Stable Transistors. *J. Am. Chem. Soc.* **2010**, *132*, 11437−11439.
(33) Bronstein, H.; Leem, D. S.; Hamilton, R.; Woebkenberg, P.; King, S.; Zhang, W.; Ashraf, R. S.; Heeney, M.; Anthopoulos, T. D.; Mello, J. D.; McCulloch, I. Indacenodithiophene-co-benzothiadiazole Copolymers for High Performance Solar Cells or Transistors via Alkyl Chain Optimization. *Macromolecules* **2011**, *44*, 6649−6652.
(34) Chen, H.; Hurhangee, M.; Nikolka, M.; Zhang, W.; Kirkus, M.; Neophytou, M.; Cryer, S. J.; Harkin, D.; Hayoz, P.; Abdi-Jalebi, M.; McNeill, C. R.; Sirringhaus, H.; McCulloch, I. Dithiopheneindenofluorene (TIF) Semiconducting Polymers with Very High Mobility in Field-Effect Transistors. *Adv. Mater.* **2017**, *29*, 1702523.
(35) Chen, H.; Wadsworth, A.; Ma, C.; Nanni, A.; Zhang, W.; Nikolka, M.; Luci, A. M. T.; Perdigão, L. M. A.; Thorley, K. J.; Cendra, C.; Larson, B.; Rumbles, G.; Anthopoulos, T. D.; Salleo, A.; Costantini, G.; Sirringhaus, H.; McCulloch, I. The Effect of Ring Expansion in Thienobenzo[b]indacenodithiophene Polymers for Organic Field-Effect Transistors. *J. Am. Chem. Soc.* **2019**, *141*, 18806−18813.
(36) Cheng, P.; Li, G.; Zhan, X.; Yang, Y. Next-generation organic photovoltaics based on non-fullerene acceptors. *Nat. Photonics* **2018**, *12*, 131−142.
(37) Wadsworth, A.; Moser, M.; Marks, A.; Little, M. S.; Gasparini, N.; Brabec, C. J.; Baran, D.; McCulloch, I. Critical review of the molecular design progress in non-fullerene electron acceptors towards commercially viable organic solar cells. *Chem. Soc. Rev.* **2019**, *48*, 1596−1625.
(38) Bristow, H.; Jacoutot, P.; Scaccabarozzi, A. D.; Babics, M.; Moser, M.; Wadsworth, A.; Anthopoulos, T. D.; Bakulin, A.; McCulloch, I.; Gasparini, N. Nonfullerene-Based Organic Photodetectors for Ultrahigh Sensitivity Visible Light Detection. *ACS Appl. Mater. Interfaces* **2020**, *12*, 48836−48844.
(39) Bristow, H.; Thorley, K. J.; White, A. J. P.; Wadsworth, A.; Babics, M.; Hamid, Z.; Zhang, W.; Paterson, A. F.; Kosco, J.; Panidi, J.; Anthopoulos, T. D.; McCulloch, I. Impact of Nonfullerene Acceptor Side Chain Variation on Transistor Mobility. *Advanced Electronic Materials* **2019**, *5*, 1900344.
(40) Holliday, S.; Ashraf, R. S.; Wadsworth, A.; Baran, D.; Yousaf, S. A.; Nielsen, C. B.; Tan, C.-H.; Dimitrov, S. D.; Shang, Z.; Gasparini, N.; Alamoudi, M.; Laquai, F.; Brabec, C. J.; Salleo, A.; Durrant, J. R.; McCulloch, I. High-efficiency and air-stable P3HT-based polymer solar cells with a new non-fullerene acceptor. *Nat. Commun.* **2016**, *7*, 11585.
(41) Wadsworth, A.; Nielsen, C.; Holliday, S.; McCulloch, I.; Kirkus, M.; Baran, D.; Ashraf, S. Preparation of organic ternary blends containing non-fullerene electron acceptors and their use in optical and electronic devices. WO2017191466 A1, 2017.
(42) Moser, M.; Thorley, K. J.; Moruzzi, F.; Ponder, J. F.; Maria, I. P.; Giovannitti, A.; Inal, S.; McCulloch, I. Highly selective chromoionophores for ratiometric Na+ sensing based on an oligoethyleneglycol bridged bithiophene detection unit. *J. Mater. Chem. C* **2019**, *7*, 5359−5365.
(43) Matsidik, R.; Komber, H.; Sommer, M. Rational Use of Aromatic Solvents for Direct Arylation Polycondensation: C-H Reactivity versus Solvent Quality. *ACS Macro Lett.* **2015**, *4*, 1346−1350.
(44) Hayashi, S.; Koizumi, T. Chloride-promoted Pd-catalyzed direct C-H arylation for highly efficient phosphine-free synthesis of π-conjugated polymers. *Polym. Chem.* **2015**, *6*, 5036−5039.
(45) Bura, T.; Morin, P.-O.; Leclerc, M. En Route to Defect-Free Polythiophene Derivatives by Direct Heteroarylation Polymerization. *Macromolecules* **2015**, *48*, 5614−5620.
(46) Wakioka, M.; Nakamura, Y.; Montgomery, M.; Ozawa, F. Remarkable Ligand Effect of P(2-MeOC6H4)3 on Palladium-Catalyzed Direct Arylation. *Organometallics* **2015**, *34*, 198−205.
(47) Wakioka, M.; Ichihara, N.; Kitano, Y.; Ozawa, F. A Highly Efficient Catalyst for the Synthesis of Alternating Copolymers with Thieno[3,4-c]pyrrole-4,6-dione Units via Direct Arylation Polymerization. *Macromolecules* **2014**, *47*, 626−631.
(48) Leclerc, M.; Brassard, S.; Beaupré, S. Direct (hetero)arylation polymerization: toward defect-free conjugated polymers. *Polym. J.* **2020**, *52*, 13−20.
(49) Iizuka, E.; Wakioka, M.; Ozawa, F. Mixed-Ligand Approach to Palladium-Catalyzed Direct Arylation Polymerization: Effective Prevention of Structural Defects Using Diamines. *Macromolecules* **2016**, *49*, 3310−3317.
(50) Wakioka, M.; Torii, N.; Saito, M.; Osaka, I.; Ozawa, F. Donor-Acceptor Polymers Containing 4,8-Dithienylbenzo[1,2-b:4,5-b′]-dithiophene via Highly Selective Direct Arylation Polymerization. *ACS Applied Polymer Materials* **2021**, *3*, 830−836.
(51) Jones, A. L.; De Keersmaecker, M.; Pelse, I.; Reynolds, J. R. Curious Case of BiEDOT: MALDI-TOF Mass Spectrometry Reveals Unbalanced Monomer Incorporation with Direct (Hetero)arylation Polymerization. *Macromolecules* **2020**, *53*, 7253−7262.
(52) Lawton, S. S.; Warr, D.; Perdigão, L. M. A.; Chang, Y.; Pron, A.; Costantini, G.; Haddleton, D. M. Determining the sequence and backbone structure of "semi-statistical" copolymers as donor-acceptor polymers in organic solar cells. *Sustainable Energy & Fuels* **2020**, *4*, 2026−2034.
(53) Warr, D. A.; Perdigão, L. M. A.; Pinfold, H.; Blohm, J.; Stringer, D.; Leventis, A.; Bronstein, H.; Troisi, A.; Costantini, G. Sequencing conjugated polymers by eye. *Science Advances* **2018**, *4*, No. eaas9543.
(54) Xiao, M.; Kang, B.; Lee, S. B.; Perdigão, L. M. A.; Luci, A.; Warr, D. A.; Senanayak, S. P.; Nikolka, M.; Statz, M.; Wu, Y.; Sadhanala, A.;

Schott, S.; Carey, R.; Wang, Q.; Lee, M.; Kim, C.; Onwubiko, A.; Jellett, C.; Liao, H.; Yue, W.; Cho, K.; Costantini, G.; McCulloch, I.; Sirringhaus, H. Anisotropy of Charge Transport in a Uniaxially Aligned Fused Electron-Deficient Polymer Processed by Solution Shear Coating. *Adv. Mater.* **2020**, *32*, 2000063.

(55) Gu, K.; Onorato, J.; Xiao, S. S.; Luscombe, C. K.; Loo, Y.-L. Determination of the Molecular Weight of Conjugated Polymers with Diffusion-Ordered NMR Spectroscopy. *Chem. Mater.* **2018**, *30*, 570−576.

(56) Zhang, X.; Bronstein, H.; Kronemeijer, A. J.; Smith, J.; Kim, Y.; Kline, R. J.; Richter, L. J.; Anthopoulos, T. D.; Sirringhaus, H.; Song, K.; Heeney, M.; Zhang, W.; McCulloch, I.; DeLongchamp, D. M. Molecular origin of high field-effect mobility in an indacenodithiophene-benzothiadiazole copolymer. *Nat. Commun.* **2013**, *4*, 2238.

(57) Tsuchiya, K.; Ogino, K. Catalytic oxidative polymerization of thiophene derivatives. *Polym. J.* **2013**, *45*, 281−286.

(58) Blaskovits, J. T.; Leclerc, M. C-H Activation as a Shortcut to Conjugated Polymer Synthesis. *Macromol. Rapid Commun.* **2019**, *40*, 1800512.

(59) Venkateshvaran, D.; Nikolka, M.; Sadhanala, A.; Lemaur, V.; Zelazny, M.; Kepa, M.; Hurhangee, M.; Kronemeijer, A. J.; Pecunia, V.; Nasrallah, I.; Romanov, I.; Broch, K.; McCulloch, I.; Emin, D.; Olivier, Y.; Cornil, J.; Beljonne, D.; Sirringhaus, H. Approaching disorder-free transport in high-mobility conjugated polymers. *Nature* **2014**, *515*, 384−388.

(60) Kline, R. J.; McGehee, M. D.; Kadnikova, E. N.; Liu, J.; Fréchet, J. M. J.; Toney, M. F. Dependence of Regioregular Poly(3-hexylthiophene) Film Morphology and Field-Effect Mobility on Molecular Weight. *Macromolecules* **2005**, *38*, 3312−3319.

(61) Zen, A.; Pflaum, J.; Hirschmann, S.; Zhuang, W.; Jaiser, F.; Asawapirom, U.; Rabe, J. P.; Scherf, U.; Neher, D. Effect of Molecular Weight and Annealing of Poly(3-hexylthiophene)s on the Performance of Organic Field-Effect Transistors. *Adv. Funct. Mater.* **2004**, *14*, 757−764.

(62) Zhang, G.; Zhao, J.; Chow, P. C. Y.; Jiang, K.; Zhang, J.; Zhu, Z.; Zhang, J.; Huang, F.; Yan, H. Nonfullerene Acceptor Molecules for Bulk Heterojunction Organic Solar Cells. *Chem. Rev.* **2018**, *118*, 3447−3507.

(63) Moser, M.; Wadsworth, A.; Gasparini, N.; McCulloch, I. Challenges to the Success of Commercial Organic Photovoltaic Products. *Adv. Energy Mater.* **2021**, *11*, 2100056.

https://doi.org/10.1021/acsmaterialslett.1c00478
ACS Materials Lett. 2021, 3, 1503−1512